Nanocrystalline $NiMoO_4$ with an Ordered Mesoporous Morphology as Potential Material for Rechargeable Thin Film Lithium Batteries

Jan Haetge,[a] Igor Djerdj,[b] and Torsten Brezesinski*[a,c]

Electronic Supplementary Information

Experimental methods

Materials

$MoCl_5$ (99.99 %), $NiCl_2{\cdot}6H_2O$ (99.99 %), $LiClO_4$ (battery grade, 99.99 %), ethanol, and 2-methoxyethanol were purchased from Sigma-Aldrich. $H[(CH_2CH_2)_{0.67}(CH_2CHCH_2CH_3)_{0.33}]_{89}$-$(OCH_2CH_2)_{79}OH$, referred to as KLE (A. Thomas, H. Schlaad, B. Smarsly, M. Antonietti, *Langmuir* 2003, **19**, 4455; B. Smarsly, D. Grosso, T. Brezesinski, N. Pinna, C. Boissiere, M. Antonietti, C, Sanchez, *Chem. Mater.* 2004, **16**, 2948), was used as the structure-directing agent.

Synthesis of mesoporous $NiMoO_4$ thin films

In a water-free container, 40 mg of KLE dissolved in a mixture of 1.0 mL of ethanol and 1.0 mL of 2-methoxyethanol is combined with both 98 mg of $NiCl_2{\cdot}6H_2O$ and 112 mg of $MoCl_5$. Once the solution is homogeneous, thin films can be produced via dip-coating on polar substrates, including SnO_2:F (FTO) glass and Si(100) wafer. Optimal conditions include withdrawal rates of 1-10 mm/s and relative humidities of (12 ± 2) %. For best results, the samples are first aged at 250 °C for 12 h and then annealed in air using a 30 min ramp to 550 °C.

Characterization

Transmission electron microscopy (TEM) and scanning electron microscopy (SEM) images were taken with a CM30-ST microscope from Philips and a LEO Gemini 982, respectively. Wide-angle X-ray diffraction (WAXD) measurements were carried out on an X'Pert PRO

diffractometer from PANalytical instruments. Grazing incidence small-angle X-ray scattering (GISAXS) patterns were collected at the German synchrotron radiation facility HASYLAB at DESY on beamline BW4 using a MarCCD area detector and a sample-detector distance of ~1820 mm. X-ray photoelectron spectroscopy (XPS) data were acquired on a VersaProbe PHI 5000 Scanning ESCA Microprobe from Physical Electronics with monochromatic Al-Kα X-ray source and a hemispherical electron energy analyzer. The electron takeoff angle to the sample surface was adjusted to 54°. The C1s signal from adventitious hydrocarbon at 284.8 eV was used as the energy reference to correct for charging. The samples were also analyzed by time-of-flight secondary ion mass spectrometry (TOF-SIMS) using a TOF-SIMS 5 from ION-TOF GmbH. A beam of 25 keV Bi^+ focused to a 60 µm spot was used to generate secondary ions for analysis. Sputter etching was carried out using a beam of 1 keV O^+ focused to a 170 µm spot. Krypton physisorption measurements were conducted at 87 K using the Autosorb-1-MP automated gas adsorption station from Quantachrome Corporation. The film thickness was determined with an Alpha Step IQ Surface Profiler from KLA Tencor. For Rietveld refinement, the software FULLPROF was used. Electrochemical experiments were carried out in an argon filled JACOMEX glove box (O_2 < 0.5 ppm, H_2O < 1 ppm) in a three-electrode cell using an Autolab PGSTAT302 potentiostat. A lithium foil several times the area of the working electrode was used as the counter electrode; the reference electrode was a lithium wire. The electrolyte solution was 1.0 mol/L $LiClO_4$ in propylene carbonate. Both cyclic voltammetry and galvanostatic charge/discharge experiments were carried out to study the electrochemical behavior using cutoff voltages at 3.5 V and 1.5 V vs. Li/Li^+. The weight was calculated by directly measuring the thickness and porosity of the thin film materials.

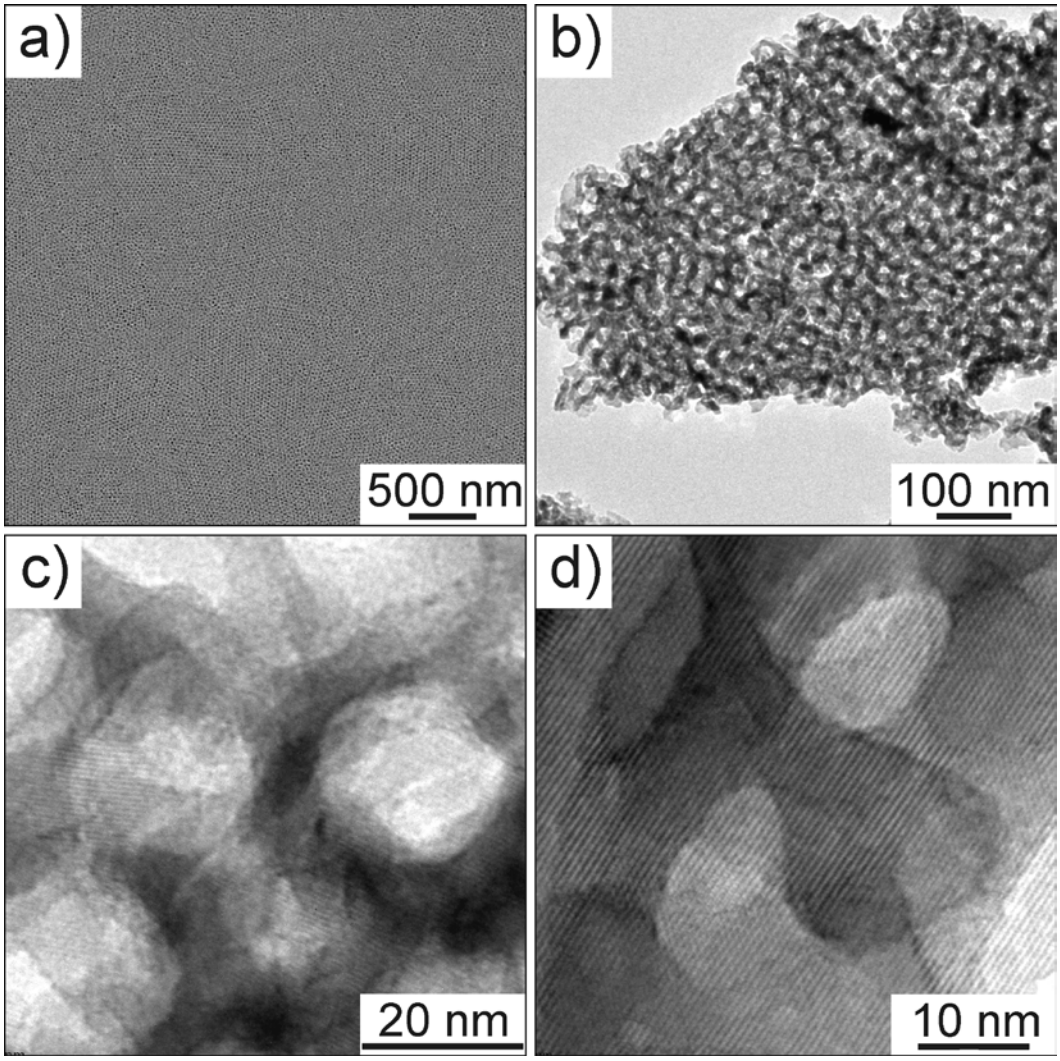

Figure S1. Electron microscopy data of mesoporous $NiMoO_4$ thin films heated to 550 °C. (a) Low-magnification SEM image. (b, c) Bright-field TEM images at different magnifications. (d) HRTEM image showing the (110) lattice planes of α-$NiMoO_4$. It can be clearly seen from these data that (1) larger structural defects can be ruled out, (2) the materials studied in this work are well-defined at both the nanoscale and the microscale, and (3) that they remain crack-free on the micrometer length scale after crystallization.

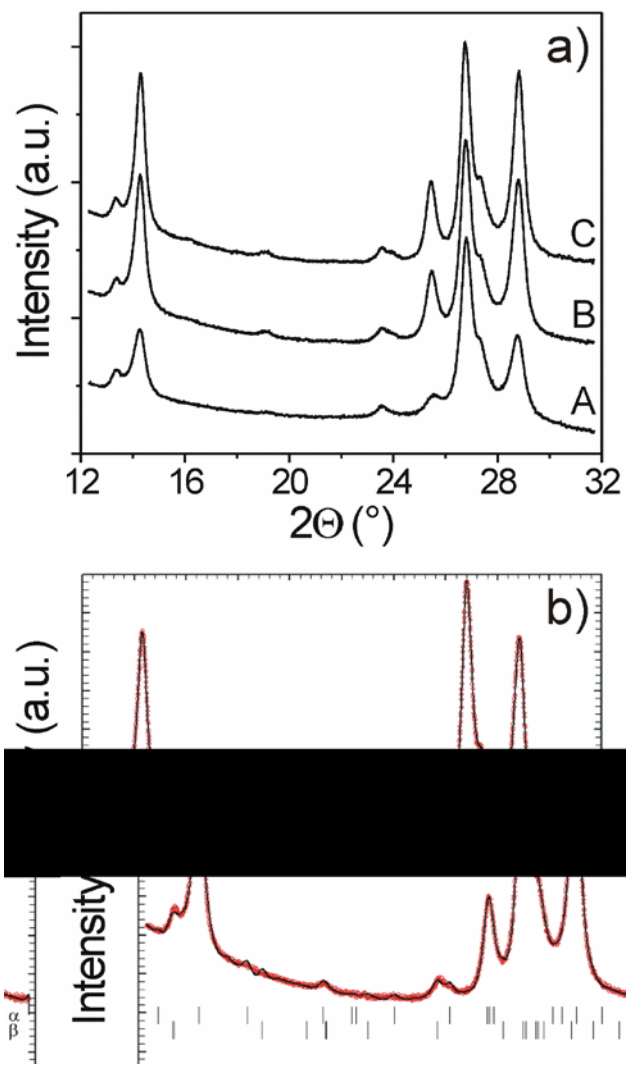

Figure S2. (a) WAXD patterns obtained on mesoporous $NiMoO_4$ thin films heated to 500 °C (A), 550 °C (B), and 600 °C (C). (b) Rietveld refinement of the 550 °C data from panel (a). Measured data are shown in red, calculated in black, and the difference between both in blue. The vertical lines indicate the Bragg positions for α-$NiMoO_4$ and β-$NiMoO_4$. Table 1 summarizes both crystallographic data and refined values. The phase composition was determined from the refined values of scale factors using the approach described by Hill and Howard (R. J. Hill, C. J. Howard, *J. Appl. Crystallogr.* 1987, **20**, 467). The modified Thompson-Cox-Hastings pseudo-Voigt method, which is known to allow for facile size analysis, was

chosen as profile function. In this approach, we assumed that line broadening of the deconvoluted profile is a result of the small crystallite size only. The values of the half-width parameters, *U*, *V*, *W*, and *X*, were kept constant at values determined by using LaB_6. The background profile was modeled using a cubic interpolation of predetermined background points with refinable heights. In the final run, a total of 75 parameters were varied, including lattice parameters, atomic coordinates, background heights, profile parameters, and zero point of detector. The quality of the refinement was assessed by the values of the discrepancy factor (profile weighted residual error), R_{wp}, and the goodness-of-fit, χ^2.

Table S1. Rietveld refinement results for mesoporous $NiMoO_4$ thin films heated to 550 °C.

Phase	α-$NiMoO_4$	β-$NiMoO_4$
Space group	*C*2/*m* (12)	*C*2/*m* (12)
Lattice parameters (Å)	*a* = 9.454(2) *b* = 8.774(2) *c* = 7.598(2) β = 112.91(2)°	*a* = 10.087(1) *b* = 9.217(1) *c* = 6.957(1) β = 107.88(1)°
Cell volume (Å^3)	580.6(3)	615.6(1)
Average crystallite size (nm)	13.2	12.3
Phase composition (wt.-%)	53.4(5)	46.6(4)
R_{wp} (%)	3.45	
Goodness-of-fit, χ^2	3.78	

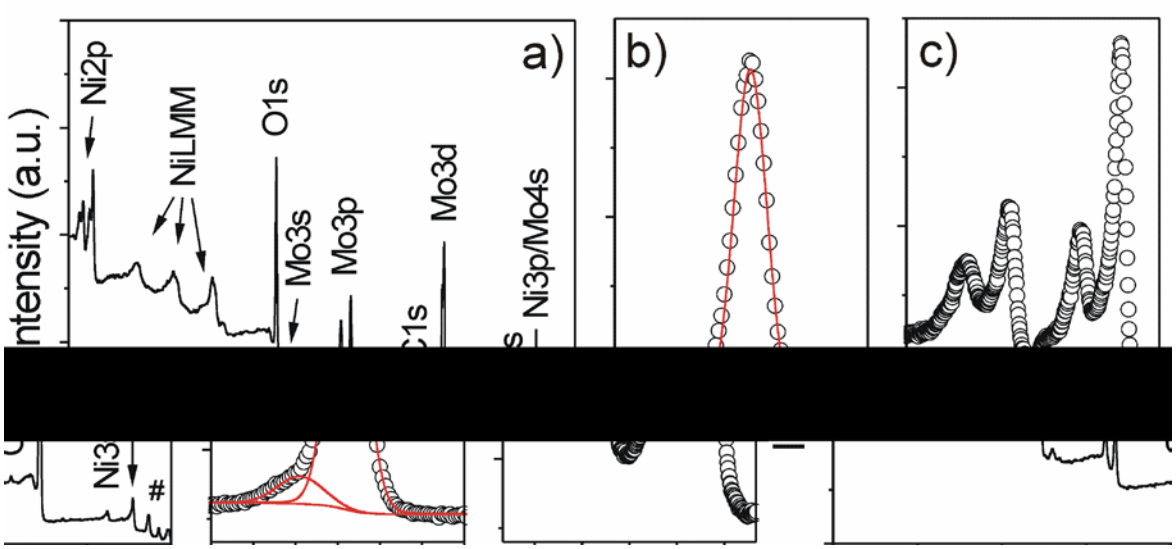

Figure S3. XPS data of mesoporous $NiMoO_4$ thin films heated to 550 °C in air. (a) Survey spectrum. The Mo 4*p* and O 2*s* regions are indicated by a hash. Apart from a very weak carbon C 1*s* peak, which we associate with adventitious hydrocarbon at the top surface, only nickel, molybdenum, and oxygen core levels are observed. (b, c) High-resolution spectra of the O 1*s* and Ni 2*p* core levels. Solid lines in red are fits to the experimental data assuming Shirley background. The O 1*s* spectrum contains one peak at a binding energy of (530.71 ± 0.05) eV and another minor one at (532.38 ± 0.05) eV. The latter component can likely be assigned to surface OH group. The Ni 2*p* spectrum is more complex and shows slightly asymmetric peaks due to the presence of both α-$NiMoO_4$ and β-$NiMoO_4$. The satellite peaks 6-7 eV higher in binding energy than the main peaks are characteristic of Ni^{2+}.

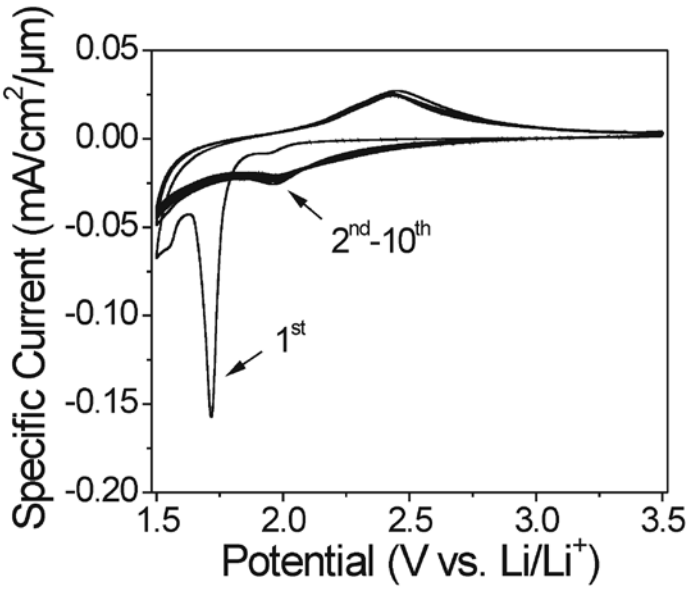

Figure S4. Voltammetry sweeps at a rate of 0.1 mV/s obtained on a mesoporous $NiMoO_4$ thin film electrode heated to 550 °C. The first 10 cycles are shown.